International Journal of Modern Manufacturing Technologies
ISSN 2067–3604, Vol. X, No. 1 / 2018

EXPERIMENTAL INVESTIGATION ON INFLUENCE OF SiC NANOPOWDER BLENDED DIELECTRIC IN ELECTRIC SPARK MACHINING

Korada Santarao[1], C.L.V.R.S.V. Prasad[2], Gurugubelli Swami Naidu[3]

[1,2]Mechanical Engineering Department, GMRIT, 532127 Andhrapradesh, India
[3] Metallurgy Engineering Department, University College of Engineering, JNTUK – Vizianagaram Campus, Dwarapudi, Vizianagaram, 535003 Andhra Pradesh, India

Corresponding author: Santarao Korada, ksantarao@gmail.com

Abstract: AISI D3 Die steel is cold worked steel manufactured for high strength and impact toughness with hardness between 54 to 61 HRC. It lacks in widespread industrial applications due to low machinability, low toughness and high resistance to softening. Electric Spark Machining (ESM) is most preferred non-conventional machining process to manufacture unique purpose tool dies, punches, etc. In the current research, an effort is made to amend AISI D3 steel's machinability by introducing SiC nanopowder in dielectric during ESM. Experiments are conducted by varying four different parameters namely powder density, peak current, pulse-on time, along with gap voltage according to the Central Composite Design (CCD) technique. Effects of these parameters were investigated on ESM response assessors such as Tool Wear Rate (TWR) along with Material Extraction Rate (MRR). Results indicated that added nanopowder to dielectric has significantly improved MRR and reduced TWR compared to the pure dielectric.

Key words: Powder-mixed ESM, silicon carbide, AISI D3 steel, material extractio rate, tool wear rate.

1. PREFACE

With the technological and industrial growth, devolvement of harder machining materials, which find broad application in automobile, aviation, medical, missile, and nuclear reactor industries has prompted the development of high strength, temperature resistant, and hard materials during last few decades. It is practically difficult to find sufficiently strong and hard tools to machine materials above at economic cutting speeds (Jain V.K., 2009). Also, machining of complex shapes in these materials with low tolerances and high surface finish by conventional methods is even more troublesome. Hence, there is an excellent demand to develop new machining technologies to cut these 'difficult-to-machine' materials with ease and precision. Among modern machining processes, electric spark machining (ESM) turned out to be very well known in manufacturing sector owing to its capability to machine any electrically conductive specimen into the desired shape with required dimensional accuracy irrespective of its mechanical strength (Ho K.H. and Newman S.T., 2003). Despite the fact that the specified machining procedure can be utilized to machine multifaceted contours without difficulty, it has specific limitations, for example, derogatory machining rate and un-satisfactory surface finish. Dielectric blending with conductive powders is one among the techniques coined to overcome the limitations. This strategy of presenting conductive particles in the dielectric fluid is acknowledged as powder blended ESM (PBESM) (Santarao K et al., 2017; Ramarao B S V et al., 2016). Jeswani M L et al., 1981 studied the impact of suspending fine Gr powder into kerosene and accomplished 60% change in MRR. Expermental results demonstrated that adding 4 g/l graphite fine particles in the dielectric increases the discharge gap for easy spark initiation and also brought down the breakdown voltage bringing about a change in machining efficiancy. Narumiya et al., (1989) utilized Si, Al and graphite powders for blending in the dielectric fluid by varying its concentration from 2 g/l to 40 g/l. Their decision demonstrated that the IEG upsurges proportionately along with the concentration of powder and this increment is higher for the aluminum powder. The preeminent surface roughness is attained for small powder concentrations. Zhao W.S. et al., (2002) made studies about the surface roughness and machining stability of PMESM using Al upto the concentration 40 g/l. They discovered that as powder concentration increases, machining efficiency was improved to 70%. The characteristics for instance size of particle, density, concentration, thermal and electrical conductivities of blended triturate significantly affect the outcomes of the PMESM process (Tzeng Yih-fong and Chen Fu-chen, 2005). Kung K Y et al., (2009) conducted experiments on

Co bonded WC specimens in dielectric together with Al triturate. They observed that the triturate particles disperse discharge energy uniformly. Jahan M P et al., (2010) investigated the possibility of enhancing the surface fineness in micro-ESM of tungsten carbide in a dielectric blended with Al, Al_2O_3, as well as Gr nanopowders . They came to the conclusion that the rise in electrical conductivity of the dielectric, ensuing expansion of discharge gap in PMESM enhances spark frequency as well as assist in easy removal of dust and debris from the machining region. Sharma S et al., (2010) reported results of conventional ESM machining performance with reverse polarity after mixing Al triturate. It is mentioned that concentration and powder characteristics have a significant effect on machining characteristics. Low density powders are able to balance surface forces considerably better enabling even distribution of particles all the way through the dielectric (Mai C et al., 2012).

Previous studies reported the results inferred adding micron-size metal (Al), nonmetallic (Gr), a metalloid (Si) powders into ESM dielectric. The literature on the use of ceramic nano powder (SiC) in ESM dielectrics is scarce, though it has high thermal conductivity compared to others. Therefore, in current research work, the influence of silicon carbide nanopowder and three ESM process parameters on two performance measures in PMESM during machining AISI D3 steel is reported.

2. EXPERIMENTAL DETAILS

2.1 Development of experimental setup

Experiments are carried out on Electronica Brand S-ZNC ESM equipment. The operating tank of machine bears a volume of 800mm X 500mm X 350mm. It really emphasizes quite a lot of nanopowder for blending to get required powder concentration in dielectric fluid for machining. Furthermore, the filtration system of the machine may possibly clog because of the presence of powder particles as well as dust and debris when making use of existing circulation system of the machine. Therefore, to address these complications, a tank, occupying three liters in volume is chosen for carrying out experiments. For proper mixing of triturate with dielectric fluid and to circulate the same in the inter electrode gap, a submerged pump is positioned in new tank. Dielectric in this tank is agitated via a stirrer to accomplish a consistent dispersion of triturate. A permanent magnet is also placed in machining receptacle to attract the specimen debris from the dielectric. The schematic representation and actual experimental setup are shown in Figure 1, Figure 2 respectively. A specially designed filtering system is incorporated to filter the dielectric for its reuse.

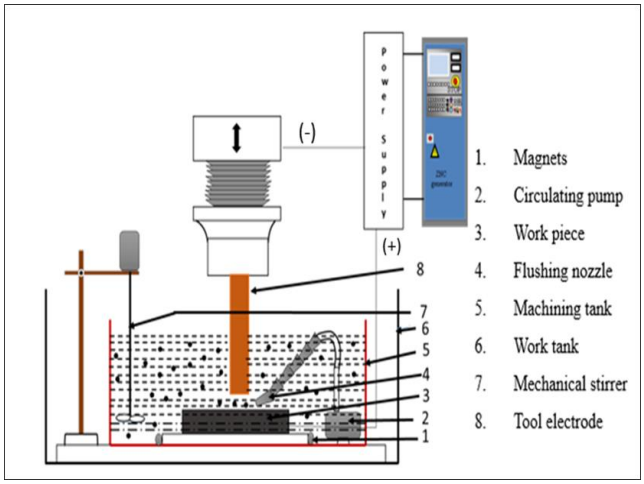

Fig. 1. Graphic representation of experimental setup

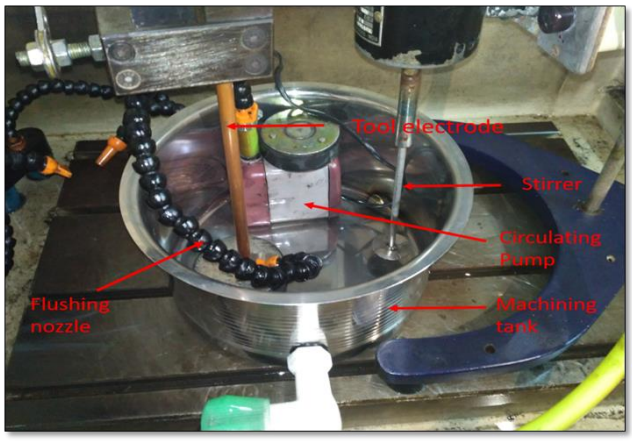

Fig. 2. Experimental setup

2.2 Selection of materials

2.2.1 Nanopowder

SiC nanopowder with typical size 50nm, as claimed by Sisco Research Laboratories Ltd, is selected in the present work due to its little density, high thermal conductivity, as well as excellent thermal shock resistance as mentioned in Table 1 and depicted in Figure 3. The XRD spectra of this powder are presented in Figure 4. Its crystallite size is determined using (1), known as, Scherer equation (Kumar V S S A I and Rao K V, 2017).

$$\psi = \frac{0.9 \times \lambda}{\beta \times \cos\theta} \quad (1)$$

where ψ, λ, β and θ represent crystallite size (nanometers), radiation wavelength, peak width at half maximum strength, and peak position respectively. The properties of Silicon Carbide nanoparticles are listed in Table 1.

2.2.2 Dielectric fluid

The dielectric fluid needs to provide an oxygen-free machining environment to prevent specimen surface layers expose to surrounded fluid which leads to the poor surface finish.

Fig. 3. As received SiC nanopowder

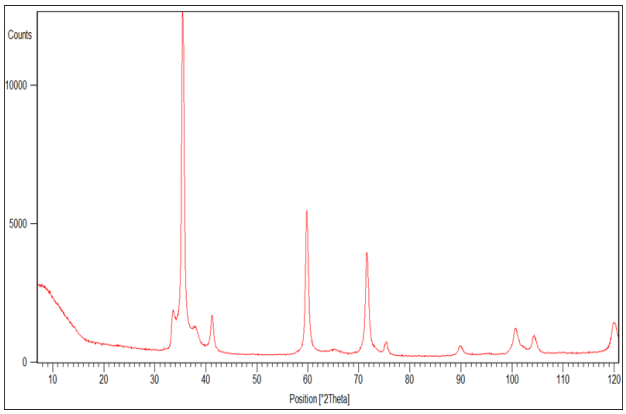

Fig. 4. XRD image of as-received SiC nanopowder

Table 1. SiC powder material properties

Property (Units)	Value
Electrical resistivity [Ω-cm]	0.001013
Thermal conductivity [W/m-K]	300
Heat of fusion [kJ/mol]	117
Specific heat [J/kg-K]	750
Melting temperature [°C]	2730
Density [g/cc]	3.21

Furthermore, it should possess higher dielectric resistance with the intention that it will not breakdown electrically too quickly until the required breakdown voltage is attained. The dielectric fluid utilized for experimentation is Electrol EDM oil. Dielectric fluid characteristics are tabulated in Table 2.

Table 2 Properties of Dielectric used

	Values
Appearance	Bright and Clear
Density @ 30 [g/cc]	0.78
Flash point [°C]	105
Pour point [°C]	-9
Viscosity @ 38°C [cSt]	2.16
Dielectric Strength [kV/m]	45

2.2.1 Workpiece and tool

AISI D3 STEEL (30mm × 30mm × 5 mm) as shown in Fig. 5 is selected as the workpiece. Cylindrical copper electrode with a diameter of 9.5 mm and length of 150 mm as presented in Figure 6 is used as an electrode because it possesses higher thermal conductivity, higher density, higher melting point.

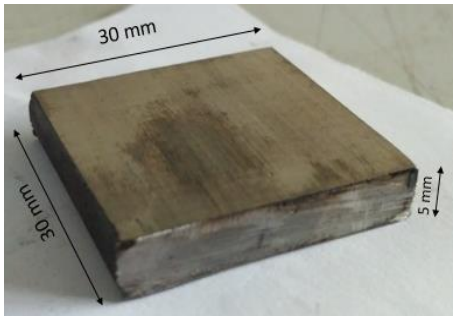

Fig. 5. AISI D3 steel workpiece

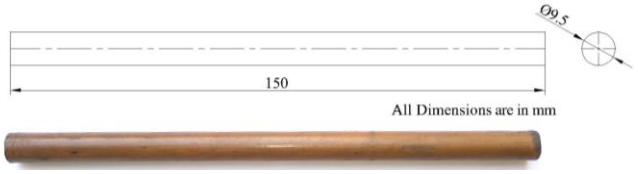

Fig. 6 Copper tool

Before machining, the workpieces and electrode were cleaned and polished. Table 3 lists mechanical properties of AISI D3 steel and electrolytic copper.

Table 3. Mechanical Properties of AISI D3 steel and copper tool

Property	Copper tool	AISI D3 steel
Thermal conductivity [W/m-K]	401	20
Density [Kg/m^3]	8960	7670
Electrical resistivity [μΩ-cm]	172	72
Specific heat [J/g°C]	0.385	0.5

2.3 Process parameters and machining conditions

Four process parameters tabulated in Table 4 are selected for the present research work. Specimen is placed in new machining tank connected to +ve terminal of power supply source during all experiments. Duty factor is set to 10 and servo's sensitivity (SEN) that governs quill's speed is set to 7 as recommended in technical manual supplied by the machine manufacturer.

Table 4. Governing factors along with levels

Parameter	Symbol	Level					Units
		-2	-1	0	1	2	
Powder concentration	C_p	0	0.2	0.4	0.6	0.8	g/l
Gap voltage	V_g	40	50	60	70	80	V
Peak current	I_p	2	4	6	8	10	A
Pulse time	T_{on}	100	200	300	400	500	μs

2.4 Design of experiments using RSM

The levels of input variables are depicted in Table 4. Each variable has five levels. Hence it would require a large number (i.e. 5^4 = 625) of combinations to assess the performance of nanopowder blended ESM. Conducting these many experiments requires much manual effort and increase the cost. To overcome these difficulties design of experiments (DoE) techniques is the best choice. It describes planning, developing as well as evaluating an experiment to ensure that valid and objective conclusions can be illustrated effectively and efficiently. The tests were executed conferring to central composite design (CCD) of response surface methodology (RSM). It provides massive information and facts from a few of experiments. It is actually a assembly of mathematical as well as statistical strategies that are helpful to model and analyze situations where responses are regulated by numerous input parameters (Kuldeep et al., 2011). For the said four input variables, experiments were carried out for 2^4 + 2 x 4 + 6 = 30 combinations of them (Table 5), according to the CCD (K M Patel et al., 2011). Each run is carried out for 20 mins and is repeated thrice to reduce measurement error. Picture of some machined test samples is displayed in Figure 7.

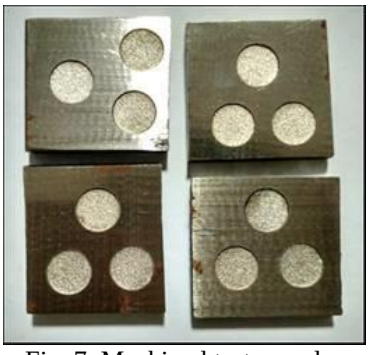

Fig. 7. Machined test samples

2.5 Performance measures

The efficiency of PMESM process is typically characterized by material removal rate (MRR) and tool wear rate (TWR). The methodology of assessing these response characteristics is discussed below.

2.5.1 Material Extraction Rate (MRR)

An Electronic digital weighing balance, having a limit up to 200 grams with an accuracy of 0.1mg as appeared in Fig. 8, was utilized for measuring the work pieces prior to and after completion of machining. After this, the MRR is calculated by using (Pavani P N L el al., 2017) (2).

$$\text{MRR (mm}^3\text{/min)} = \frac{\Delta W}{\rho_W \times t} \qquad (2)$$

where ΔW is variation in weight of the work piece (g), ρ_W is work piece density (g/mm^3), and t is the experiment duration (minutes).

2.5.2 Tool wear rate (TWR)

$$\text{TWR (mm}^3\text{/min)} = \frac{\Delta T}{\rho_T \times t} \qquad (3)$$

where ΔT is variation in weight of electrode (g), The term ρ_T is electrode density (g/mm^3), and t as mentioned in (2).

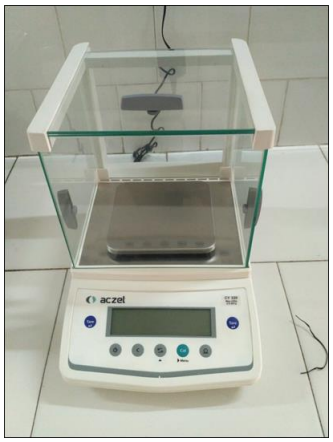

Fig. 8. Digital weighing machine

3. RESULTS AND DISCUSSION

3.1 Powder Material and ESM parameters impact on Material Removal Rate

The impact of the considered process parameters, i.e., powder concentration (Cp), peak current (Ip), pulse ON time and gap voltage on the material removal rate (MRR) of the work-piece are described within this section. Graphs were plotted to examine the process parameters influence on MRR.

Table 5. MRR and TWR for all combinations

Exp. No	C_p [g/l]	I_p [A]	T_{on} [µs]	V_g [V]	MRR [mm^3/min]	TWR [mm^3/min]
1	0.0	6	300	60	2.117	0.00168
2	0.2	4	200	50	2.055	0.00160
3	0.2	4	400	50	1.126	0.00096
4	0.2	4	200	70	1.501	0.00000
5	0.2	4	400	70	0.511	0.00041
6	0.2	8	200	50	4.597	0.00367
7	0.2	8	400	50	3.211	0.00257
8	0.2	8	200	70	4.507	0.00360
9	0.2	8	400	70	3.188	0.00254
10	0.4	2	300	60	0.977	0.00078
11	0.4	6	300	40	2.102	0.00168
12	0.4	6	100	60	3.422	0.00274
13	0.4	6	500	60	1.859	0.00148
14	0.4	6	300	60	2.145	0.00171
15	0.4	6	300	60	2.196	0.00175
16	0.4	6	300	60	2.196	0.00175

17	0.4	6	300	60	2.145	0.00171
18	0.4	6	300	60	2.196	0.00175
19	0.4	6	300	60	2.145	0.00171
20	0.4	6	300	80	2.525	0.00202
21	0.4	10	300	60	5.676	0.00454
22	0.6	4	200	50	1.695	0.00135
23	0.6	4	400	50	1.796	0.00143
24	0.6	4	200	70	2.173	0.00174
25	0.6	4	400	70	2.137	0.00170
26	0.6	8	200	50	3.037	0.00242
27	0.6	8	400	50	3.056	0.00244
28	0.6	8	200	70	4.648	0.00371
29	0.6	8	400	70	3.958	0.00316
30	0.8	6	300	60	2.787	0.00222

3.1.1 Influence of powder concentration on MRR

Improvement in MRR (Figure 9) is noticed as powder concentration increased up to 0.6g/l. Such improvement in MRR may be resulting from decrease in dielectric breakdown strength whenever conductive fine powder is added to it. Furthermore, the gap flanked by the two electrodes considerably raises in PMESM in comparison with conventional ESM. This gap rise brings about engorged discharge passages. Simultaneously, the powder particles attempt to link the discharge gap. This augments discharge dispersion which results in an improvement in sparking and therefore, MRR increases (Tzeng et al., 2005). Further increment in powder causes to 0.8g/l, a reduction in MRR is observed. The decrease of MRR after 0.6 g/l could be attributed to short circuit at higher powder density which causes the machining process to become an uneven condition to the net reduction in MRR. One more reason is that as higher quantity of powder concentration cannot be taken away quite easily from the machining gap. This is evident from the previous results (Kansal et al., 2005 and Jahan et al., 2010).

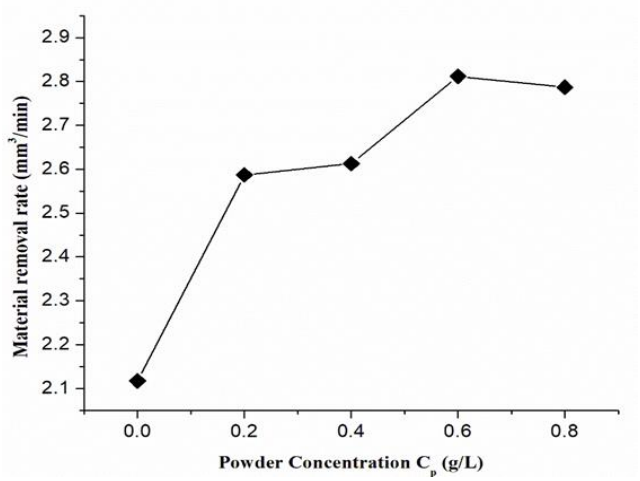

Fig. 9. Variation of MRR with powder concentration

3.1.2 Peak current effect on MRR

The behavior of MRR concerning the peak current is appeared in Fig. 10. It can be watched that the maximum MRR, 5.677mm^3/min, is gotten at the highest peak current i.e at 10A. The MRR is seen to be increased relatively to peak current. This might be on account of, the higher the current, spark intensity is increased and brings about high material removal from the surface of the work piece. A comparable trend was seen by (Kansal et al., 2007; Bai et al., 2011).

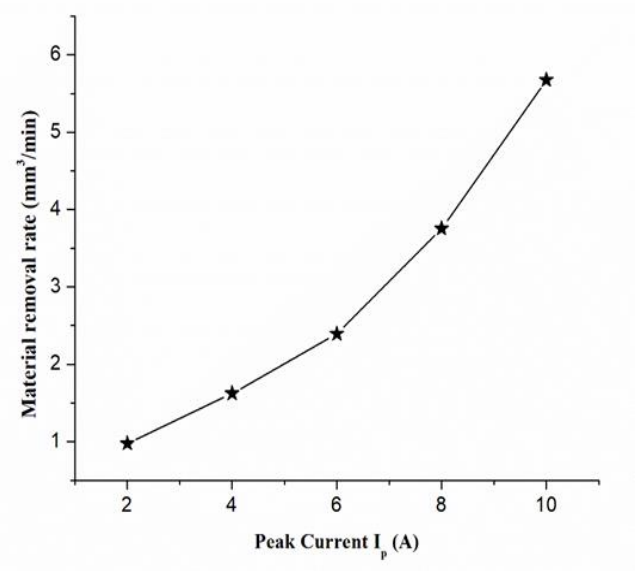

Fig. 10. Variation of MRR with peak current

3.1.3 MRR variation with respect to Pulse-ON time

It is clear from Figure 11 that the MRR diminishes with the increase in Ton within the range of investigation. The higher the pulse on time, the spark intensity is diminished because of the development of plasma channel. The high amount of heat energy prevailing in the space between two electrodes first converts work material layer by layer into liquid and then into vapour phases. Later, less weight work material in vapour phase comes out of confined space, gets cooled due to surrounding dielectric and settles as debris. Higher the Pulse-ON time, wider will be the growth of plasma channel presiding in the inter-electrode space. This wide plasma channel lessens heat energy density impinging on the work. As a result, work material that vaporises reduces and hence material extraction from work reduces.

3.1.4 MRR variation with respect to Voltage

As observed in Figure 12. MRR enhancement is observed till 70 V and further increment in gap voltage lead to a decline in MRR.

As the gap voltage increases, it causes an increase in spark energy promoting rise in MRR. Needless to say, at an elevated gap voltage, the IEG will become increased.

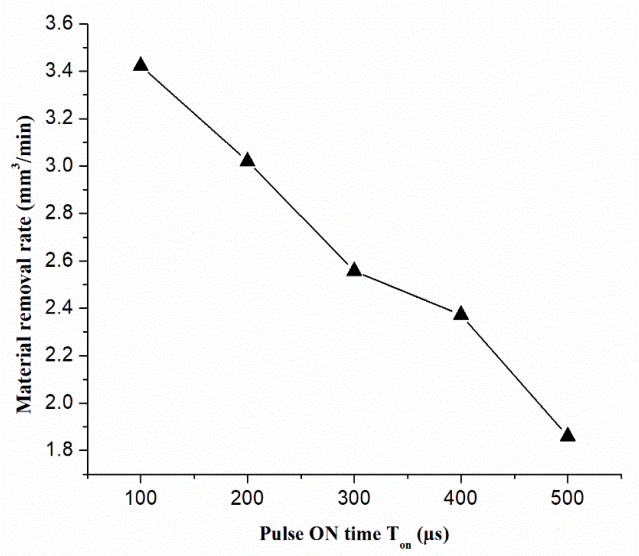

Fig. 11. Deviation in MRR with pulse on time

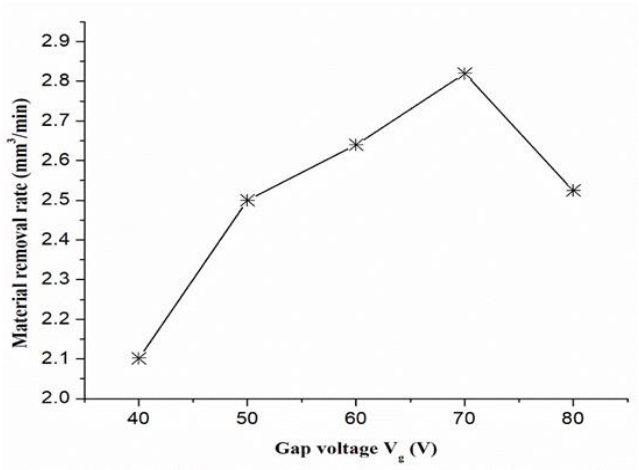

Fig. 12. MRR change with gap voltage

As a consequence, the duration of time needed to fill up the IEG with the ionized particles is expanded on account of the advancement in gap voltage. Thusly, a slight decrease in MRR was figured it out. Therefore, considering all above parameters, maximum material removal rate is seen with a high peak current of 10 A, with a pulse on time Ton of 100 µs, and a powder concentration of 0.6 g/l.

3.2 Tool Wear Rate (TWR) variation in relation to governing parameters

Tool wear is one of the important parameter as that of material removal rate. Minimizing the TWR, which designates a least possible alteration on electrode's outer periphery that leads to enhanced precision without any aberrations on machined work turned out to be an important criterion in any research.

3.2.1 Influence of powder concentration on TWR

The influence of powder concentration on TWR of the machined electrode is depicted in Figure 13.

The addition of SiC powder concentration to dielectric has a less significant effect on TWR.

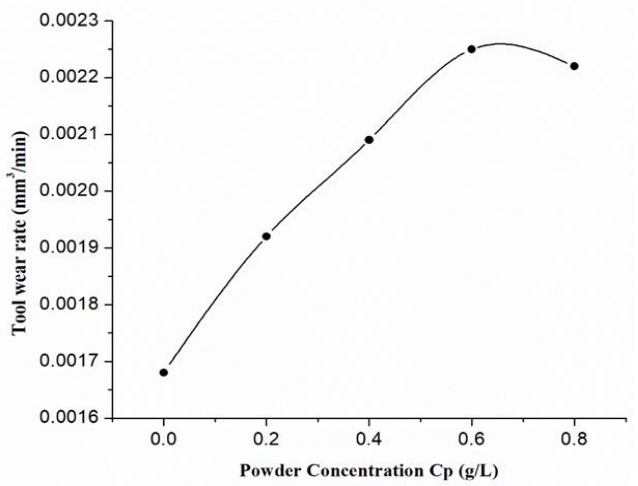

Fig. 13. Variation of TWR with powder concentration

This is due to various properties of SiC such as excellent physical, chemical, wear resistance and abrasion resistance, lower thermal expansion and high heat of fusion. However, escalation in powder concentration slightly increases the Tool wear rate. This is due to upsurge in electrical conductivity and thermal conductivity of the dielectric. The sparking frequency is increased with improved flushing of debris efficiently away from the gap as the electrical conductivity is increased. This resulted in effective discharge transitivity under the sparking area due to increase in the thermal conductivity. Thus electrode surface is exposed to more amount of heat.

3.2.2 Influence of peak current on TWR

The change in tool wear with peak current is presented in Figure 14. TWR increments with an increase in the peak current. This might be because of, with increase of current, more discharge energy is produced and ultimately, more amount of material gets melted at both tool and work piece. The measured TWR values for SiC powder-mixed dielectric was provided in Table 5.

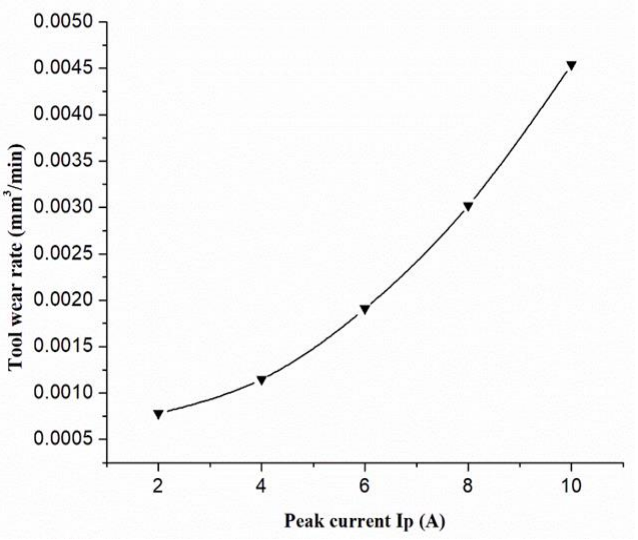

Fig. 14. Variation of TWR with peak current

3.2.3 Influence of Pulse-ON time on TWR

The impact of Pulse-On Time on TWR is illustrated in Figure 15. It is observed that the tool wear rate is diminished with an increase in pulse on time. This is because of the reason that, at too long pulse on time causes the plasma channel to grow and this extension causes less discharge energy of the surface of the electrode. As a result, less heat is developed at the tool surface. So, less volume of material is worn from tool.

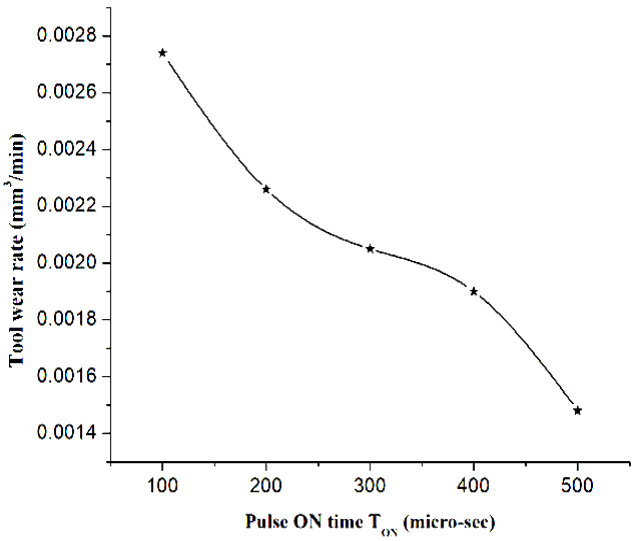

Fig. 15. TWR change with pulse ON time

3.2.4 Effect of gap voltage on TWR

The impact of gap voltage on tool wear rate is depicted in Figure 16. Gap voltage causes very less effect on TWR. As gap voltage increases, spark intensity increases resulting in the increment of TWR. However, at larger gap voltage, the inter electrode gap becomes larger. Therefore, it took some time to fill the IEG with intentionally added nano powder particles. As result, TWR declined.

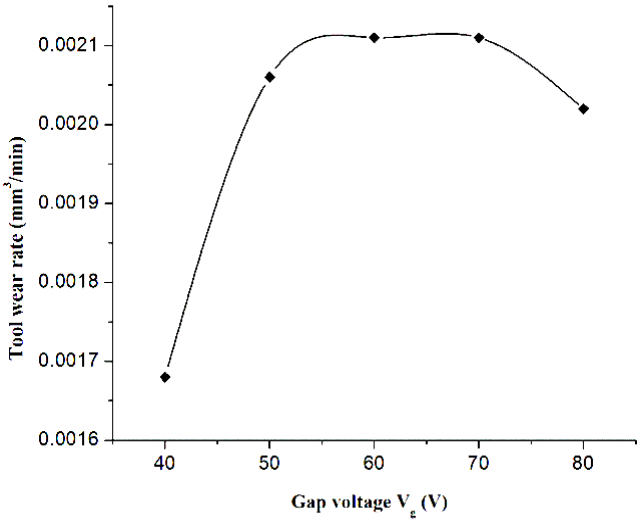

Fig. 16. TWR change with Gap voltage

4. CONCLUSION

In the present research work, the effect of PMESM governing factors on the performance assessors are presented according to the RSM-based design of experiments. MRR and TWR are the measures of productivity studied. Results evidently demonstrated noteworthy progress in terms of various performance measures for PMESM compared to ESM without powder additive. However, such improvement is dependent on characteristics of powder materials and their concentration. The following major contributions are obtained from the entire work:

-All the chosen input factors have a solid influence on MRR and TWR.

-For the powder-blended dielectric, large and shallow craters were observed at the machined work piece surface compared to conventional ESM due to the enhanced thermal and electrical conductivity of dielectric which causes an early spark generation, thus enhancing material extraction from work.

-Higher peak current is an anticipated factor to yield more material erosion from work. But it also causes more wear on tool.

-Higher pulse on time is unattractive factor for material erosion.

-Too much of gap voltage results in decreasing the MRR and TWR.

5. REFERENCE

1. Ramarao, B. S. V., Sailesh, P., Sreenivasarao, M., (2016). *A Review on Current Trends in PM-EDM using Commercial Kerosene as Di-Electric Fluid,* Int. J. Sci. Eng. Technol. Res., 5(6), 2196–2203.
2. Mai, C., Hocheng, H., Huang, S., (2012). *Advantages of carbon nanotubes in electrical discharge machining*, Int. J. Adv. Manuf. Technol., 59, 111–117.
3. Boothroyd, G., Winston, A.K., (1989). *Fundamentals of Machining and Machine Tools*, CRC Press, Taylor & Francis Group, Boca Raton.
4. Narumiya, H., (1989). *EDM by powder suspended working fluid*, Proceedings of the 9th ISEM, pp. 5–8.
5. Kansal, H.K., Singh, S., Kumar, P., (2007). *Effect of Silicon Powder Mixed EDM on Machining Rate of AISI D2 Die Steel*, J. Manuf. Process., 9(1), 13–22.
6. Kansal, H.K., Singh S., Kumar, P., (2005). *Parametric optimization of powder mixed electrical discharge machining by response surface methodology*, J. Mater. Process. Technol., 169(3), 427-436.
7. Jeswani, M.L., (1981). *Effect of the Addition of Graphite Powder to Kerosene used as the Dielectric Fluid in Electrical Discharge Machining*, Wear, 70(2), 133-139.

8. Ho, K. H., Newman, S. T., (2003). *State of the art electrical discharge machining (EDM)*, Int J Mach Tools Manuf, 43(13), 1287–1300.
9. Patel, K. M., Pandey, P. M., Rao, P. V., (2011). *Study on machinabilty of Al_2O_3 ceramic composite in edm using response surface methodology*, J. Eng. Mater. Technol., 133(2), 1–10.
10. Santarao, K., Prasad, C.L.V.R.S.V., Swaminaidu, G., (2017). *Influence of Nano and Micro Powders in Electric Discharge Machining: A Review*, J. Manuf. Technol. Res., 8(1-2), 11-20.
11. Kuang-Yuan Kung, K.Y., Horng, J.T., Chiang, K.T. (2009). *Material removal rate and electrode wear ratio study on the powder mixed electrical discharge machining of cobalt-bonded tungsten carbide*, Int. J. of adv. Eng. Technol, 40(1-2), 95-104.
12. Jahan, M.P., Rahman, M., Wong, Y.S., (2010). *Modelling and experimental investigation on the effect of nanopowder-mixed dielectric in micro-electro discharge machining of tungsten carbide*, Proc. Inst. Mech. Eng. Part B J. Eng. Manuf., 224(11), 1725– 1739.
13. Ojiha, K., Garg, R. K., Singh, K. K., (2011). *The effect of nickel micro powder suspended dielectric on EDM performance measures of EN-19 steel*, J. Eng. Appl. Sci., 6(1), 27-37.
14. Pavani, P.N.L., Pola Rao R., Santarao., K., (2017). *Performance Assessment And Mathematical Modeling Of Process Parameters In Electrical Discharge Machining Of En-31 Tool Steel Material Using Taguchi DOE*, Engineering Journal, 21(2), 227-236.
15. Sai Kumar, V.S., Rao, K.V., (2017). *Investigation of Ultrasonic Parameters Of Zno-Ethylene Glycol Nanofluids*, Journal of Ovonic Research, 13(3), 91-99.
16. Saurabh, S., Kumar, A., Beri, N., Kumar, D., (2010). *Effect of aluminium powder addition in dielectric during electric discharge machining of hastealloy on machining performance using reverse polarity*, Int. J. Adv. Eng. Technol., 1(3), 13-24.
17. Yih-Fong, T., Fu-Chen, C., (2005). *Investigation into some surface characteristics of electrical discharge machined SKD-11 using powder-suspension dielectric oil*, J. Mater. Process. Technol., 170(1–2), 385–391.
18. Jain, V.K., (2009). *Advanced machining processes*, 475-499, Allied Publishers, New Delhi.
19. Bai, X., Zhang, Q. H., Yang, T. Y., Zhang., J. H., (2013). *Research on material removal rate of powder mixed near dry electrical discharge machining*, Int. J. Adv. Manuf. Technol., 68(5-8), 1757–1766.
20. Yih-Fong, T., Fu-Chen., C. (2005). *Investigation into some surface characteristics of electrical discharge machined SKD-11 using powder-suspension dielectric oil*, J. Mater. Process. Technol., 170(1-2), 385-391.
21. Zhao, W.S., Meng, Q.G., Wang, Z.L., (2002). *The application of research on powder mixed EDM in rough machining*, J. Mater. Process. Technol., 129(1-3), 30–33.

Received: October 15, 2017 / Accepted: June 15, 2018 / Paper available online: June 20, 2018